J Ind Microbiol Biotechnol (2016) 43:691–701
DOI 10.1007/s10295-016-1743-9

GENETICS AND MOLECULAR BIOLOGY OF INDUSTRIAL ORGANISMS

A mutant form of 3-ketosteroid-Δ^1-dehydrogenase gives altered androst-1,4-diene-3, 17-dione/androst-4-ene-3,17-dione molar ratios in steroid biotransformations by *Mycobacterium neoaurum* ST-095

Minglong Shao[1] · Xian Zhang[1] · Zhiming Rao[1] · Meijuan Xu[1] · Taowei Yang[1] · Hui Li[2] · Zhenghong Xu[2] · Shangtian Yang[3]

Received: 29 November 2015 / Accepted: 29 January 2016 / Published online: 17 February 2016

Abstract *Mycobacterium neoaurum* ST-095 and its mutant *M. neoaurum* JC-12, capable of transforming phytosterol to androst-1,4-diene-3,17-dione (ADD) and androst-4-ene-3,17-dione (AD), produce very different molar ratios of ADD/AD. The distinct differences were related to the enzyme activity of 3-ketosteroid-Δ^1-dehydrogenase (KSDD), which catalyzes the $C_{1,2}$ dehydrogenation of AD to ADD specifically. In this study, by analyzing the primary structure of $KSDD_I$ (from *M. neoaurum* ST-095) and $KSDD_{II}$ (from *M. neoaurum* JC-12), we found the only difference between $KSDD_I$ and $KSDD_{II}$ was the mutation of Val^{366} to Ser^{366}. This mutation directly affected KSDD enzyme activity, and this result was confirmed by heterologous expression of these two enzymes in *Bacillus subtilis*. Assay of the purified recombinant enzymes showed that $KSDD_{II}$ has a higher $C_{1,2}$ dehydrogenation activity than $KSDD_I$. The functional difference between $KSDD_I$ and $KSDD_{II}$ in phytosterol biotransformation was revealed by gene disruption and complementation. Phytosterol transformation results demonstrated that $ksdd_I$ and $ksdd_{II}$ gene disrupted strains showed similar ADD/AD molar ratios, while the ADD/AD molar ratios of the $ksdd_I$ and $ksdd_{II}$ complemented strains were restored to their original levels. These results proved that the different ADD/AD molar ratios of these two *M. neoaurum* strains were due to the differences in KSDD. Finally, KSDD structure analysis revealed that the $Val^{366}Ser$ mutation could possibly play an important role in stabilizing the active center and enhancing the interaction of AD and KSDD. This study provides a reliable theoretical basis for understanding the structure and catalytic mechanism of the Mycobacteria KSDD enzyme.

Keywords *Mycobacterium neoaurum* · Phytosterol · 3-Ketosteroid-Δ^1-dehydrogenase · Mutation

Abbreviations

AD	Androst-4-ene-3,17-dione
ADD	Androst-1,4-diene-3,17-dione
KSDD	3-Ketosteroid-Δ^1-dehydrogenase
FAD	Flavin adenine dinucleotide
Me-β-CD	Methyl-β-cyclodextrin
PMS	Phenazine methosulphate
DCPIP	2,6-Dichlorophenolindophenol

Introduction

As the second largest category drugs after antibiotics, steroid drugs play an important role in treating and preventing various diseases. Since 1952 when Murray and Peterson [17] discovered the process of 11α-hydroxylation of progesterone by *Rhizopus nigricans*, the production of steroid drugs by microbial technology has attracted the attentions of many microbiologists. When compared with the traditional chemical synthesis process, microbial transformation of steroid compounds has the advantages of yielding products of high purity at low cost and under environmentally

✉ Zhiming Rao
raozhm@jiangnan.edu.cn

[1] Laboratory of Applied Microorganisms and Metabolic Engineering, School of Biotechnology, Jiangnan University, 1800 Lihu Avenue, Wuxi, Jiangsu 214122, People's Republic of China

[2] Laboratory of Pharmaceutical Engineering, School of Pharmaceutical Sciences, Jiangnan University, Wuxi, Jiangsu 214122, People's Republic of China

[3] Department of Chemical and Biomolecular Engineering, The Ohio State University, Columbus, OH 43210, USA

friendly conditions [5]. Over the past half century, numerous microbial transformations of steroid compounds, including steroid hydroxylation, Δ^1-dehydrogenation and sterol side chain cleavage, have been reported [4]. Among these studies, microbial sterol side chain cleavage has received much attention in the pharmaceutical industry, and has become an important pathway to produce many steroid intermediates [11]. Since the discovery that microorganisms could degrade the side chain of sterols to produce 17-ketosterols [12], mainly androst-4-ene-3,17-dione (AD) and androst-1,4-diene-3,17-dione (ADD), phytosterol has become a major raw material in pharmaceutical industry for its low cost, abundant availability, and the efficiency of its transformation into steroid intermediates [13]. Among the products of microbial side chain cleavage obtained from phytosterol, AD and ADD are important and valuable steroid drug intermediates, widely used for the commercial production of mineralocorticoids, corticosteroids, oral contraceptives, and other pharmaceutical steroids [33].

Many microbial strains have been described as biocatalysts of sterol bioconversions and different approaches for steroid microbial conversion have been applied [4]. For example, it has been reported that the bioconversion of cholesterol to ADD could be enhanced by the addition of lecithin, with a final ADD yield of 59 % (w/w) [27]. Wang et al. reported that resting cell biotransformation of phytosterol to ADD in a cloud point system could improve ADD production with yields up to 12 g/L [26]. Shen et al. showed that use of hydroxypropyl-β-cyclodextrin (HP-β-CD) as a cosolvent could increase AD and ADD yield with phytosterol as the substrate [23]. In our recent study of phytosterol biotransformation by *M. neoaurum*, we proposed a three-stage fermentation strategy for enhancing ADD production with methyl-β-cyclodextrin (Me-β-CD) used as cosolvent [21].

In the process of phytosterol biotransformation, 3-ketosteroid-Δ^1-dehydrogenase (KSDD) is the key enzyme that catalyzes the conversion of AD to ADD [33]. During microbial steroid transformations, both AD and ADD are formed. As the only structural difference between AD and ADD is the $C_{1,2}$ double bond [33], so the structures of AD and ADD are highly similar. This high structural similarity greatly increases the cost of the downstream processes for the separation and purification of AD from ADD [28]. Therefore, it is crucial to obtain strains capable of efficient transformation of phytosterol into AD and ADD with as high ADD/AD or AD/ADD ratios as possible.

Wild-type *M. neoaurum* ST-095 (formerly *Mycobacterium* sp.), typically produces an ADD/AD molar ratio of 1:2 when used for phytosterol biotransformation [34]. In our previous study, mutant strain *M. neoaurum* ZADF-4 was isolated [9], which gave AD/ADD molar ratios of 8:1 when used for steroid biotransformations, but activity was reduced [9]. By analyzing the DNA sequence of the mutant *ksdd* gene, a nine nucleotide deletion and two point mutations were revealed, which resulted in amino acid changes [9]. To develop steroid biotransformation systems capable of producing high AD/ADD or ADD/AD ratios and while retaining high levels of biotransformation activity, it is necessary to understand the behavior of the key enzyme KSDD [29]. As a flavin adenine dinucleotide (FAD)-dependent enzyme, KSDD not only catalyzes the conversion of AD to ADD, but also plays an important role in microbial sterol catabolism as well as other steroid drug transformations [15, 24]. However, the catalysis mechanism of *Mycobacterium* KSDD enzymes is not well resolved, and structural information on KSDD is still limited. Previous studies focused on the investigation of the molecular, catalytic and spectral characteristics of KSDD from different strains, and based on chemical modification, mutagenesis, and kinetics experiments, several key amino acid residues were identified [6, 14]. In a recent study, Rohman et al. revealed the first structure and catalytic mechanism of the KSDD enzyme from *Rhodococcus erythropolis* SQ1 [19]. They confirmed that the enzyme contains two domains: an FAD-binding domain and a catalytic domain, and they also found that the active site contains four key residues: Tyr^{119}, Tyr^{318}, Tyr^{487}, and Gly^{491}. Xie et al. further reported that Ser^{138} was a key amino acid residue of KSDD and changes at that position led to large differences in the ADD/AD ratio [29].

By UV-NTG mutation, *M. neoaurum* JC-12 (formerly *Mycobacterium* sp.-11), a strain capable of producing an ADD/AD molar ratio of 10:1, was derived from strain *M. neoaurum* ST-095 [34]. Furthermore, total amounts of ADD and AD produced by these two strains were the same. Having shown that KSDD enzyme activity directly affects ADD/AD molar ratios, we investigated the KSDDs from *M. neoaurum* ST-095 (named $KSDD_I$) and *M. neoaurum* JC-12 (named $KSDD_{II}$) to attempt to explain the different characteristics of these two strains. After searching the Protein Data Bank (PDB) database for structural similarity, we found that $KSDD_I$ and $KSDD_{II}$ have the highest similarity to KSDD from *R. erythropolis* SQ1 [29].

In this study, by sequence alignment, we found that the only difference between $KSDD_I$ and $KSDD_{II}$ was the mutation of Val^{366} to Ser^{366}. The enzymatic characteristics of $KSDD_I$ and $KSDD_{II}$ were studied by heterologous expression in *Bacillus subtilis* 168, and the results revealed that the mutation of Val^{366} to Ser^{366} enhanced KSDD enzyme activity. We further investigated the function of $KSDD_I$ and $KSDD_{II}$ in AD and ADD production by gene disruption and complementation, which confirmed that the different characteristics of these two *M. neoaurum* strains with respect to ADD/AD molar ratios attained were caused by this mutation. The mechanism

responsible for the different characteristics of $KSDD_I$ and $KSDD_{II}$ was further unraveled at the molecular level by modeling the complex structure of KSDD-AD. The results suggested that the change of Val^{366} to Ser^{366} in KSDD could facilitate the interaction of KSDD with AD and thereby enhance KSDD enzyme activity. This study not only serves as a basis for further studies on the structural analysis and catalytic mechanism of this dehydrogenase, but also provides a reliable theoretical basis for site-directed mutagenesis to further improve ADD/AD molar ratios in future research.

Materials and methods

Strains, plasmids and primers

The strains, plasmids and primers used in this work are listed in Table 1.

Reagents, media and cultivation

The AD and ADD standards were purchased from Sigma-Aldrich (Shanghai, China). Substrate phytosterol (95 % purity) was obtained from Wuhan Kaidi Fine Chemical Industrial Co., Ltd. (Wuhan, China). Tryptone and yeast extract were purchased from Oxoid Ltd. (Basingstoke Hampshire, England). Methyl-β-cyclodextrin (Me-β-CD) was obtained from Zhiyuan Biotechnology Co., Ltd (Shandong, China). Methanol and ethyl acetate obtained from Jiangsu Hanbon Science & Technology CO., Ltd. (Jiangsu, China) were chromatographic grade. All other chemicals and reagents were analytical grade and purchased from Sinopharm Chemical Reagent Co., Ltd. (Shanghai, China), unless otherwise stated.

Escherichia coli and *B. subtilis* were cultivated in Luria Broth (LB) medium and were used as the cloning and expression hosts, respectively. The cultivation of *M. neoaurum* ST-095 and *M. neoaurum* JC-12 was performed according to our previous study [21].

Expression and purification of KSDD in *B. subtilis* 168

Both the $ksdd_I$ and $ksdd_{II}$ genes were cloned with the forward primer P1 and the reverse primer P2, from the genome DNA of *M. neoaurum* ST-095 and *M. neoaurum* JC-12, respectively. The plasmids pMA5-$ksdd_I$ and pMA5-$ksdd_{II}$ were constructed by inserting the $ksdd_I$ and $ksdd_{II}$ genes into the *Bam*H I and *Nde* I sites of pMA5. The transformation of *B. subtilis* cells was in accordance with the procedure described by Anagnostopoulos et al. [1], and the selection of the recombinant strains $BS168_I$ and $BS168_{II}$ followed the process described in our previous study [20].

After cultivation in 50 mL LB medium for 24 h, recombinant cells were harvested by centrifugation (10,000 rpm, 10 min and 4 °C) and washed twice with 50 mM Tris–HCl buffer (pH 7.0). Then the harvested cells were resuspended with 5 mL Tris–HCl buffer. After ultrasonic disruption, cell debris was removed by centrifugation at 10,000 rpm and 4 °C for 30 min. The supernatant was then used for enzyme activity assays, SDS-PAGE analysis and enzyme purification. Enzyme purification was carried out using HisTrap™ HP columns according to the manufacturer's instructions [30].

Enzyme activity assay of KSDD

The KSDD enzyme activity was determined spectrophotometrically at 30 °C←using phenazine methosulphate (PMS) and 2,6-dichlorophenolindophenol (DCPIP). Reaction mixtures (1 mL) contained 50 mM Tris–HCl buffer (pH 7.0), 1.5 mM PMS, 40 μM DCPIP, appropriate volumes of the supernatant or cell extract, and 200 mM AD in methanol (2 %) [33]. KSDD activity is expressed as U/mg of protein, and 1 U is defined as the amount of enzyme giving a reduction of 1 μmol/min DCPIP ($\xi_{600} = 11.3 \times 10^3$/cm/M) [28].

Kinetic parameters of $KSDD_I$ and $KSDD_{II}$ were performed in 50 mM Tris–HCl buffer (pH 7.0) at 30 °C by changing the concentration of the substrate (AD). Kinetic parameters (K_m, V_{max} and k_{cat}) were determined by fitting a plot of rate versus substrate concentration to the Michaelis–Menten equation using nonlinear regression in the software GraphPad Prism 5.0 (GraphPad Software, Inc. La Jolla, CA, USA).

AD and phytosterol transformation analysis

The conversion of AD by the purified enzymes was done in 50-mL shake flasks and the transformation system was similar to the enzyme assay system. The reaction mixture (10 mL) consisted of 50 mM Tris–HCl buffer (pH 7.0), 1.5 mM PMS, 40 μM DCPIP, appropriate amounts of the purified enzymes and 10 mg AD in methanol (2 %). The conversion was carried out at 30 °C and 160 rpm for 12 h. Phytosterol transformation was carried out in 250-mL shake flasks and was performed as described in our previous study [21].

The *ksdd* gene disruption and complementation

Gene deletion in *M. neoaurum* was performed as described by Gordhan and Parish with minor modifications [7]. To delete the $ksdd_I$ and $ksdd_{II}$ genes, a 425 bp upstream sequence and a 350 bp downstream sequence were amplified by PCR with primers P3/P4 and P5/P6. Then the two

Table 1 The strains, plasmids and primers used in this work

Name	Description	Sources
Strains		
Escherichia coli		
E. coli JM109	*recA1, endA1, gyrA96, thi-1, hsd R17*(r_k^- m_k^+)*supE44*	Invitrogen
$JM109_I$	*E. coli* JM109 containing pMA5-$ksdd_I$	This study
$JM109_{II}$	*E. coli* JM109 containing pMA5-$ksdd_{II}$	This study
Bacillus subtilis		
B. subtilis 168	*trpC2*	Laboratory stock
$BS168_E$	*B. subtilis* 168 containing pMA5 as a control	This study
$BS168_I$	*B. subtilis* 168 containing pMA5-$ksdd_I$	This study
$BS168_{II}$	*B. subtilis* 168 containing pMA5-$ksdd_{II}$	This study
Mycobacterium neoaurum		
M. neoaurum ST-095	Source of $ksdd_I$ gene	Laboratory stock
M. neoaurum JC-12	Source of $ksdd_{II}$ gene	Laboratory stock
Mut_{ksddI}	$ksdd_I$-deleted mutant of *M. neoaurum* ST-095	This study
Mut_{ksddII}	$ksdd_{II}$-deleted mutant of *M. neoaurum* JC-12	This study
$Comp_{ksddI}$	$ksdd_I$-complemented strain of Mut_{ksddII}	This study
$Comp_{ksddII}$	$ksdd_{II}$-complemented strain of Mut_{ksddI}	This study
Plasmids		
pMD18-T	*E. coli* clone vector; Amp^R	Takara
pMA5	*HpaII* promoter, colE1 ori, *repB*, replicates in *E. coli* (Amp^R) or *B. subtilis* (Km^R)	Laboratory stock
pMA5-$ksdd_I$	pMA5 containing $ksdd_I$-His	This study
pMA5-$ksdd_{II}$	pMA5 containing $ksdd_{II}$-His	This study
p2 NIL	Recombination vector of *mycobacterium*; Km^R	Dr. Parish
pGOAL19	*Hyg* Pag_{85}-*lacZ* P_{hsp60}-*sacB*, *Pac*I cassette vector; Amp^R	Dr. Parish
pMV261	Shuttle vector of *E. coli* and *mycobacterium*, carrying the heat-shock promoter *hsp*60; Km^R	Dr. W.R. Jacobs Jr.
pMV306	Mycobacterial integrating vector, Km^R	Dr. W.R. Jacobs Jr.
p2N-Δ*ksdd*	p2NIL harboring a crossover PCR product which covers the flanking regions of $ksdd_I$ or $ksdd_{II}$ gene and the selection cassette from pGOAL19; Km^R and Hyg^R	This study
p261-*ksdd*	pMV261 carrying the $ksdd_I$ or $ksdd_{II}$ gene; Km^R	This study
p306-*ksdd*	pMV306 carrying the $ksdd_I$ or $ksdd_{II}$ gene under the *hsp*60 promoter; Km^R	This study
Primers 5′–3′		
P1	CGGGATCCATGTTCTACATGACTGCCC	
P2	CGCATATGTCA**GTGGTGGTGGTGGTGGTG**GGCCTTTCCAGCGAG	
P3	CGGGATCCATGTTCTACATGACTGCCC	
P4	CCCATCCACTAAACTTAAACACGTCGGGACCGAGCTTC	
P5	TGTTTAAGTTTAGTGGATGGGCCACCATCGAACGGTTC	
P6	CCCAAGCTTTCAGGCCTTTCCAGCGAG	

The restriction enzyme sites were underlined, and the His-Tag coding region was bold typed

Amp^R ampicillin resistant, *Km^R* kanamycin resistant

purified fragments were mixed to be used as template to amplify a single large fragment using primers P3/P6. The amplification products (containing the upstream and downstream regions of $ksdd_I$ and $ksdd_{II}$, 775 bp) were digested with *Kpn*I and *Hin*dIII and cloned into the plasmid p2 NIL to construct recombinant plasmid p2 N-Δ$ksdd_I$ and p2 N-Δ$ksdd_{II}$ which also included a selectable marker gene cassette, which was removed from pGOAL19 by digestion using *Pac*I and then inserted into the *Pac*I site of p2 NIL. Finally, after alkali treatment and UV irradiation, the plasmids p2N-Δ$ksdd_I$ and p2N-Δ$ksdd_{II}$ were transformed into *M. neoaurum* ST-095 and *M. neoaurum* JC-12 by electrotransformation, respectively [7]. Prospective deletion mutants of $ksdd_I$ and $ksdd_{II}$ were confirmed by PCR and gene sequencing, and named Mut_{ksddI} and Mut_{ksddII}, respectively.

Plasmid pMV306 was employed as an integrating expression vector to prepare plasmids for complementation of the deleted mutants of $ksdd_I$ and $ksdd_{II}$. To construct the complementation plasmids, we first constructed plasmids p261-$ksdd_I$ and p261-$ksdd_{II}$. Using primers P1/P6, $ksdd_I$ and $ksdd_{II}$ genes were obtained through PCR techniques. Then $ksdd_I$ and $ksdd_{II}$ were inserted into the *Bam*H I/*Hind* III sites of plasmid pMV261 to create plasmids p261-$ksdd_I$ and p261-$ksdd_{II}$, respectively. Then expression cassettes containing $ksdd_I$ and $ksdd_{II}$ under the control of the heat-shock promoter *hsp*60 were removed from plasmids p261-$ksdd_I$ and p261-$ksdd_{II}$, respectively, by double digestion with *Xba*I/*Cla*I, and subsequently inserted into the corresponding sites of pMV306 to obtain the complementation plasmids p306-$ksdd_I$ and p306-$ksdd_{II}$. The plasmids p306-$ksdd_I$ and p306-$ksdd_{II}$ were further transferred into Mut_{ksddII} and Mut_{ksddI} by electrotransformation to generate the KSDD complemented strains $Comp_{ksddI}$ and $Comp_{ksddII}$, respectively.

Analytical methods

The methods used for structural analysis of $KSDD_I$ and $KSDD_{II}$ were in accordance with our recent report [10]. The structural models of $KSDD_I$ and $KSDD_{II}$ were acquired by homology modeling using SWISS-MODEL Workspace (http://swissmodel.expasy.org/). Analysis of the three-dimensional structures of the $KSDD_I$ and $KSDD_{II}$ enzymes were conducted using Discovery Studio 2.5 software.

The preparation and analysis of biotransformation products were performed as follows: 1 mL of sample was withdrawn from culture broth and extracted with 4 ml of ethyl acetate. After centrifugation, 2 ml of the supernatant was analyzed on a Shimadzu HPLC instrument equipped with a C18 column (Diamonsil ®C18, 5 μm particles, 250 mm × 4.6 mm) and a UV/visible detector. ADD and AD were detected at 240 nm and the mobile phase consisted of methanol and water (70/30, v/v). The flow rate was 1 mL/min and the column temperature was 30 °C [21, 22].

Results and discussion

Sequence analysis of $KSDD_I$ and $KSDD_{II}$

Using the *ksdd* gene sequence from *M. neoaurum* NwIBL-01 (Gene ID: 251736854) as the basis, we designed the primers P1/P2 (Table 1) to obtain the complete *ksdd* gene sequence from *M. neoaurum* ST-095 and *M. neoaurum* JC-12 by PCR techniques. Both the $ksdd_I$ and $ksdd_{II}$ gene fragments were complete open reading frames and contained 1701 bp nucleotides. Rohman et al. have reported that the four key amino acid residues in the active center of KSDD from R. *erythropolis* SQ1 are Tyr^{119}, Tyr^{318}, Tyr^{487}, and Gly^{491}, and so we determined the corresponding amino acid residues of KSDD from *M. neoaurum* by sequence alignment (Fig. 1). As shown in Fig. 1, by the amino acid sequence alignment analysis, we predicted the key amino acid residues in the active center of KSDD from *M. neoaurum* were Tyr^{125}, Tyr^{365}, Tyr^{541}, and Gly^{545}. By further analysis of the nucleotide sequences of $ksdd_I$ and $ksdd_{II}$, we found the $ksdd_I$ and $ksdd_{II}$ genes showed 99.9 % similarity, and there were only two differences located at nucleotides 1096 and 1097 (Fig. 2a), which caused the Val^{366} of $KSDD_I$ to change into Ser^{366} of $KSDD_{II}$ (Fig. 2b). Mutations in the amino acid sequence of KSDD have been shown previously to lead to changes in KSDD structure, which resulted in different enzyme activities [29]. Therefore, we speculated that the residue change from Val^{366} to Ser^{366} might have enhanced KSDD enzyme activity, and thereby increased the ADD/AD molar ratio. Similar results have also been reported in studies on *Mycobacterium* sp. VKM Ac-1816D and *Mycobacterium* sp. VKM Ac-1815D, where a single point mutation apparently led to differences in accumulation of the main product [2].

Enzymatic characteristics of $KSDD_I$ and $KSDD_{II}$

To confirm that the differences in KSDD activity were caused by amino acid differences between $KSDD_I$ and $KSDD_{II}$, the $ksdd_I$ and $ksdd_{II}$ genes, together with 6 His-tag coding regions appended at their 3′-termini, were expressed in *B. subtilis* 168. The KSDD enzyme activity of the recombinant strains was detected and the results are shown in Table 2. $BS168_I$ and $BS168_{II}$ showed KSDD activities of 0.65 and 1.72 U/mg, respectively. No enzyme activity was

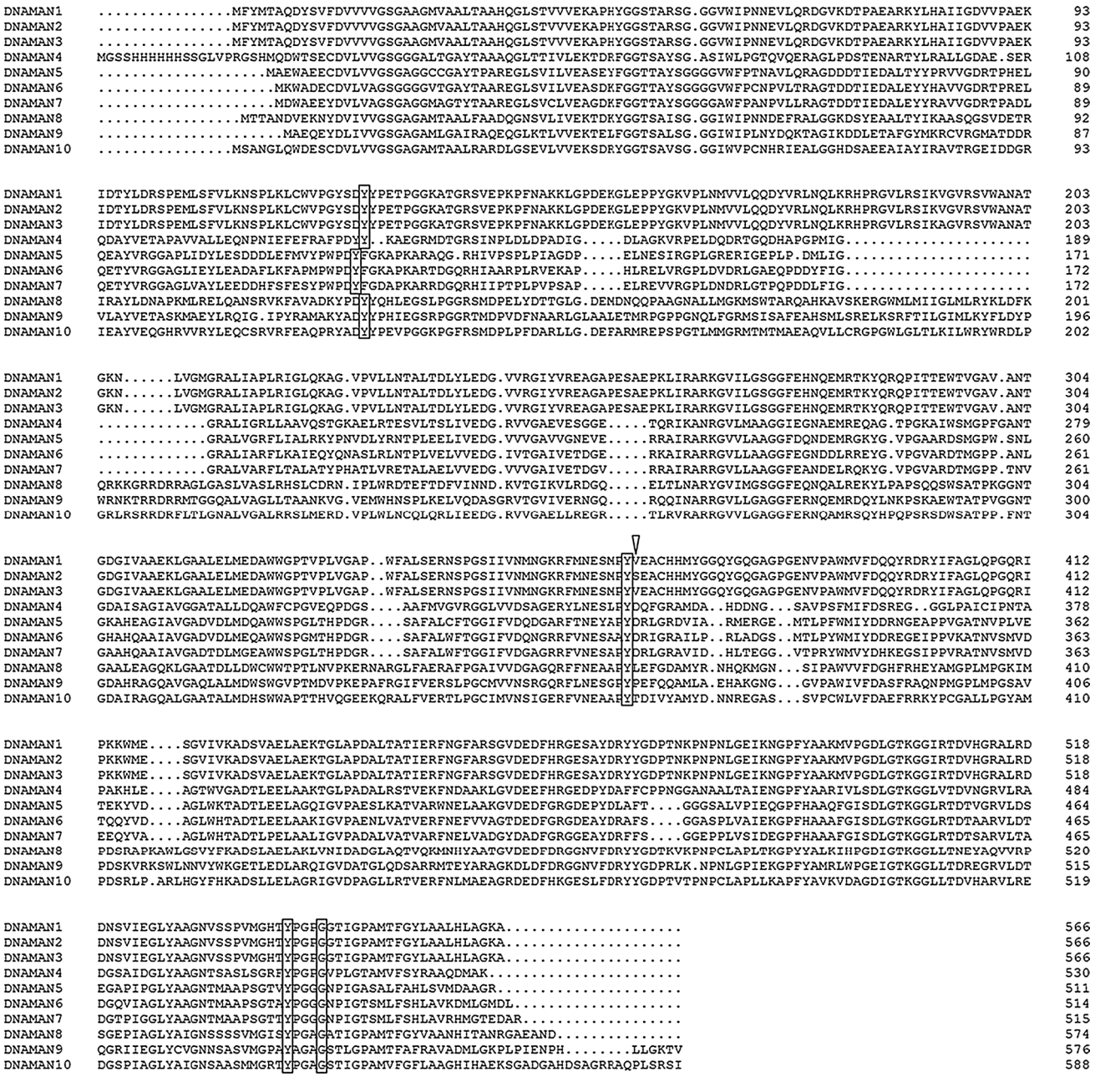

Fig. 1 Sequences alignment of KSDD from different strains. The key residues in the active center were marked with *black frames* and the mutation site (Ser^{366}) was indicated by *hollow inverted triangle*. GenBank accession numbers for KSDD were in brackets: DNAMAN1, $KSDD_I$; DNAMAN2, $KSDD_{II}$; DNAMAN3, KSDD from *M. neoaurum* NwIBL-01 (ACT10280.1); DNAMAN4, KSDD from R. *erythropolis* SQ1 (ABW74859.1); DNAMAN5, KSDD from *R. rhodochrous* (BAA22789.1); DNAMAN6, KSDD from *M. fortuitum* (ALI25697.1); DNAMAN7, KSDD from *Pimelobacter simplex* (AIY19527.1); DNAMAN8, KSDD from *Pseudoalteromonas haloplanktis* TAC125 (CAI87189.1); DNAMAN9, KSDD from *Comamonas testosteroni* (BAP91417.1); DNAMAN10, KSDD from *Pseudomonas resinovorans* NBRC 106553 (BAN46966.1)

detected in $BS168_E$. These results gave preliminary indication that the enzyme activity of $KSDD_{II}$ was higher than that of $KSDD_I$.

Recombinant $KSDD_I$ and $KSDD_{II}$ were then purified using HisTrap™ HP columns to yield products with the expected molecular weight of about 61 kDa, as shown by SDS-PAGE analysis in Fig. 3. Enzyme activity and Michaelis–Menten kinetics of the purified KSDD were measured at 30 °C and pH 7.0 with AD as substrate. As shown in Table 3, the specific activity of $KSDD_{II}$ (4.03 U/mg) was much higher than that of $KSDD_I$ (1.46 U/mg) indicating that the mutation of Val^{366} to Ser^{366} greatly

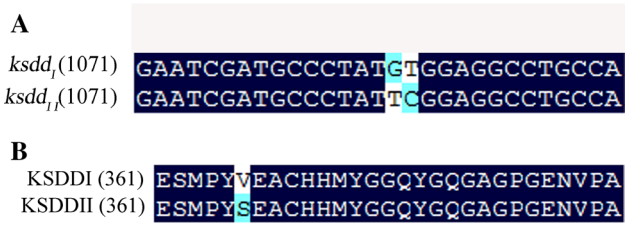

Fig. 2 Alignment analysis of the nucleotide sequence (**a**) and amino acid sequence (**b**)

Table 2 The KSDD enzyme activity of different strains

Strains	Enzyme activity[a] (U/mg)
$BS168_E$	n.d.
$BS168_I$	0.65 ± 0.03
$BS168_{II}$	1.72 ± 0.06

All assays were performed in triplicate with three independent measurements. Standard deviations of the biological replicates were represented by *error bars*

n.d. not detected enzyme activity

[a] One unit of enzyme activity was defined as the amount of enzyme required to reduce 1 μmol DCPIP at 30 °C and pH 7.0 per min

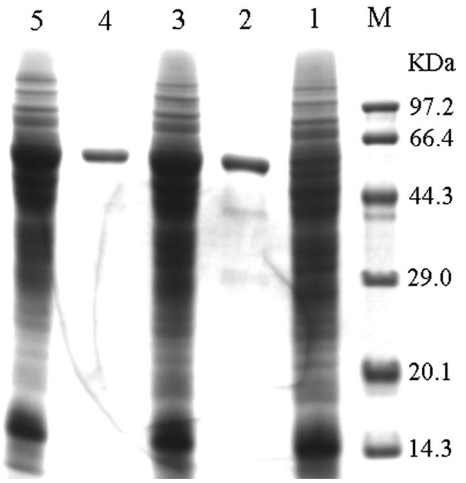

Fig. 3 SDS-PAGE analysis of $KSDD_I$ and $KSDD_{II}$ expression in recombinant *B. subtilis*. *Lanes*: *Lane M* Protein marker; *Lane 1* crude cell extracts of $BS168_E$ as a control; *Lane 2* purified $KSDD_I$; *Lane 3* crude cell extracts of $BS168_I$; *Lane 4* purified $KSDD_{II}$; *Lane 5* crude cell extracts of $BS168_{II}$

improved the KSDD enzyme activity. The Michaelis constant (K_m value) of $KSDD_{II}$ was lower than that of $KSDD_I$ suggesting that the AD affinity of KSDD was increased by the Val^{366} to Ser^{366} mutation. The k_{cat}/K_m value of $KSDD_{II}$ (0.53 μM^{-1} min^{-1}) was higher than that of $KSDD_I$ (0.07 μM^{-1} min^{-1}), which further showed that the catalytic efficiency of $KSDD_{II}$ was improved considerably. Finally,

Table 3 Enzyme kinetic parameters of purified KSDD

Enzymes	K_m (μM)	K_{cat} (min^{-1})	K_{cat}/K_m (μM^{-1} min^{-1})	Specific activity[a] (U/mg)
$KSDD_I$	34	2.39	0.07	1.46
$KSDD_{II}$	11	5.78	0.53	4.03

[a] One unit of enzyme activity was defined as the amount of enzyme required to reduce 1 μmol DCPIP at 30 °C and pH 7.0 per min

the conversion of AD to ADD by the purified enzymes, $KSDD_I$ and $KSDD_{II}$, was investigated. As shown in Fig. 4, AD transformation was catalyzed more efficiently by $KSDD_{II}$ than by $KSDD_I$ indicating the $KSDD_{II}$ enzyme activity was higher than $KSDD_I$. Since concentrations of $KSDD_I$ and $KSDD_{II}$ enzymes added into the conversion system were the same, we conclude that the major factor that leads to the difference in KSDD enzyme activity is the amino acid differences in the two forms of KSDD enzyme.

Phytosterol degradation into AD and ADD by mycobacteria is complicated and the metabolic pathway remains unresolved. However, KSDD has been identified as a key enzyme in the metabolic pathway for many years [28]. Since Plesiat et al. successfully heterologous expressed the KSDD from *Pseudomonas testosterone* in *E. coli* in 1991 [18], the *ksdd* genes from different species, such as *Arthrobacter*, *Rhodococcus* and *Mycobacterium*, were heterologously expressed in different hosts including *E. coli*, *B. subtilis*, *Streptomyces lividans*, etc. [3, 8, 16, 33]. These previous studies of KSDD mainly focused on heterologous expression and molecular characterization. Recently, Rohman et al. provided the first crystal structure and identified the key active site residues of the KSDD enzyme from *R. erythropolis* [19]. Xie et al. also found that Ser^{138} was a critical amino acid in the KSDD enzyme from *M. neoaurum* [29]. Despite all these studies, the structure and catalytic mechanism of the KSDD enzyme from *M. neoaurum* were still unclear. In the present study, we heterologously expressed the $KSDD_I$ and $KSDD_{II}$ from *M. neoaurum* in *B. subtilis* 168 to reveal their enzymatic characteristics. Our results indicate that the mutation of Val^{366} to Ser^{366} appears to improve KSDD affinity toward AD and enhance KSDD enzyme activity. This study suggests possible directions for future site-directed mutagenesis studies of KSDD to improve its enzyme activity.

The function of $KSDD_I$ and $KSDD_{II}$ in phytosterol biotransformation

To eliminate the possible impact of other factors on the different ADD/AD molar ratios in *M. neoaurum* ST-095 and *M. neoaurum* JC-12, the $ksdd_I$ and $ksdd_{II}$ genes were disrupted and then complemented to clarify their function

in phytosterol conversion. The cell growth curves showed that there were no differences in biomass and residual glucose between the *ksdd* gene disrupted strains and the parent strains (Fig. 5), which indicated that *ksdd* gene disruption has no observable effect on the growth of *M. neoaurum* under these conditions. The results of phytosterol transformation by the parent strains, *ksdd* gene disrupted strains, and *ksdd* gene complemented strains are shown in Fig. 6. As seen in Fig. 6, with the disruption of *ksdd* in *M. neoaurum* ST-095 and *M. neoaurum* JC-12, ADD production decreased markedly, while AD accumulation increased. The ADD/AD molar ratios of the mutant strains Mut_{ksddI} and Mut_{ksddII} were almost the same (1:29), but production levels were very low. Then the mutant strains Mut_{ksddI} and Mut_{ksddII} were complemented with $ksdd_{II}$ and $ksdd_{I}$ to construct the complemented strains $Comp_{ksddI}$ and $Comp_{ksddII}$, respectively. As a result, the ADD/AD molar ratio of the complemented strain $Comp_{ksddI}$ returned to a level very similar to that of *M. neoaurum* JC-12, while the ADD/AD molar ratio of the complemented strain $Comp_{ksddII}$ was similar to that of *M. neoaurum* ST-095 (Fig. 6). Xie et al. [29] reported that disruption of *ksdd* in *M. neoaurum* MNR M3 led to the strain completely losing KSDD activity and that no ADD was detected. In this study, *ksdd* gene disruption caused ADD production to decrease dramatically. However, there was still a small amount of ADD detected during the

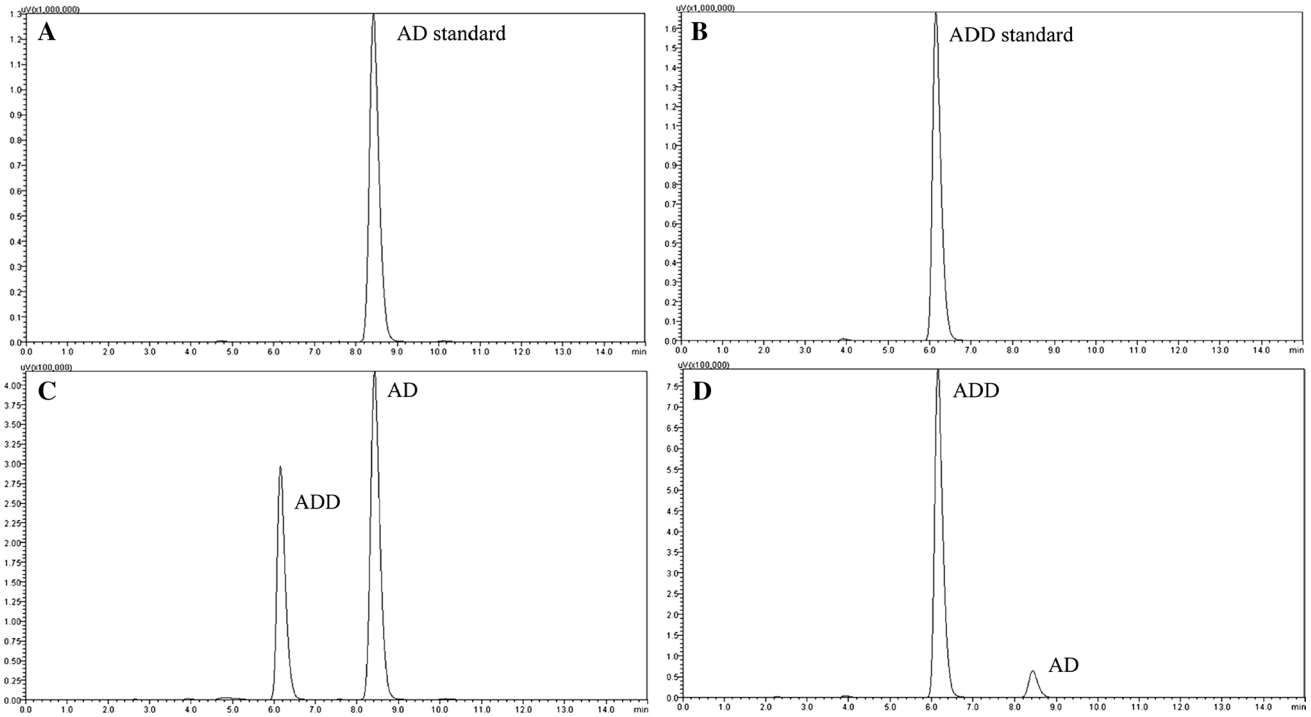

Fig. 4 HPLC analysis of AD transformation. **a** The standard sample of AD; **b** the standard sample of ADD; **c** AD transformed sample by purified $KSDD_I$; **d** AD transformed sample by purified $KSDD_{II}$

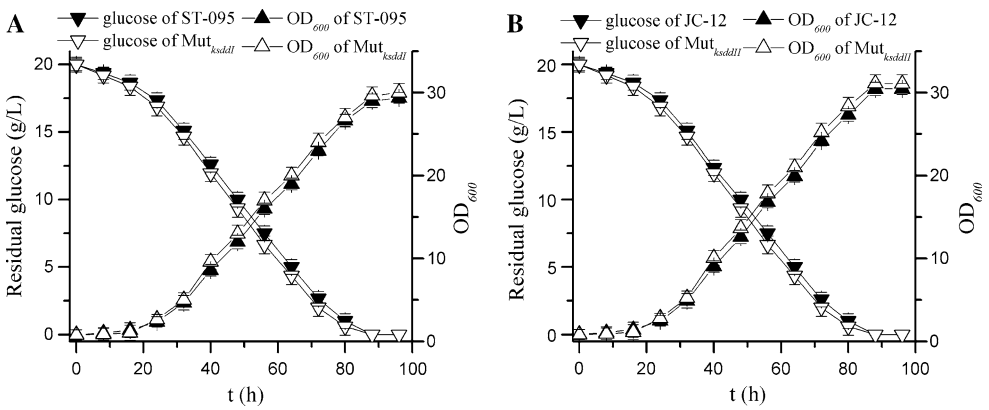

Fig. 5 The cell growth curves of the parent strains and their *ksdd* gene disrupted mutants. **a** *M. neoaurum* ST-095 and Mut_{ksddI}; **b** *M. neoaurum* JC-12 and Mut_{ksddII}. All assays were performed in triplicate with three independent measurements. Standard deviations of the biological replicates were represented by *error bars*

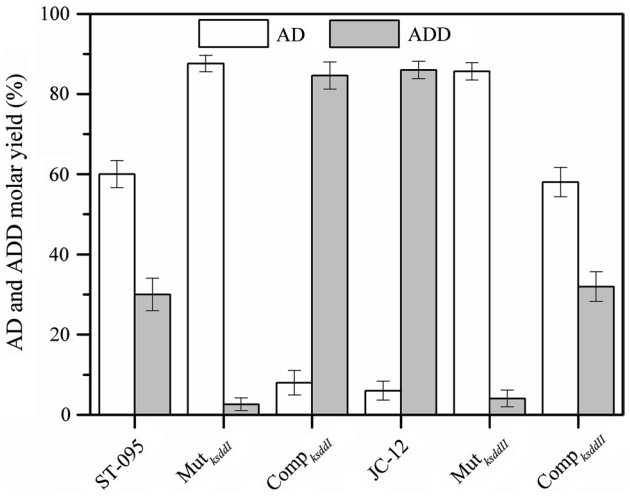

Fig. 6 AD and ADD molar yields of the engineered *M. neoaurum* strains. The transformation was carried out for 7 days with 10 g/L phytosterol as substrate. The phytosterol was not completely converted to AD and ADD, and the AD and ADD molar yield was not up to 100 %. The balance is essentially unconverted phytosterol. All assays were performed in triplicate with three independent measurements. Standard deviations of the biological replicates were represented by *error bars*

phytosterol conversion, and this result was in accordance with that reported by Wei et al. [28]. This phenomenon may be explained by the possible presence of other enzymes that possess $C_{1,2}$ dehydrogenation ability [32]. All of these results suggest that the most reasonable explanation for the difference in the ADD/AD molar ratios and KSDD enzyme activities between *M. neoaurum* ST-095 and *M. neoaurum* JC-12 is that the amino acid residue difference in 366 position considerably influences KSDD activity.

Structure analysis of $KSDD_I$ and $KSDD_{II}$

As the amino acid residues play important roles in enzyme structure and catalytic reactions, single amino acid mutations can significantly influence enzyme activity [29]. The structure of $KSDD_I$ and $KSDD_{II}$ was modeled using the crystal structure of KSDD (3-ketosteroid-Δ^1-dehydrogenase from *R. erythropolis* SQ1, PDB entry 4c3x; 43.1 % sequence identity) as template. The resulting models were used to explain the differences in enzyme catalytic efficiency between $KSDD_I$ and $KSDD_{II}$ in terms of structure using the software of Discovery Studio 2.5 according to our recent report [10]. The analysis of the three-dimensional structure of the wild-type $KSDD_I$ revealed the extremely hydrophobic environment of the active center (Fig. 7a). Molecular docking of complexes KSDD-AD with the active site of KSDD obtained from *M. neoaurum* JC-12 (with 43.1 % sequence identity of KSDD from *R. erythropolis* SQ1, PDB entry 4c3x) was performed by

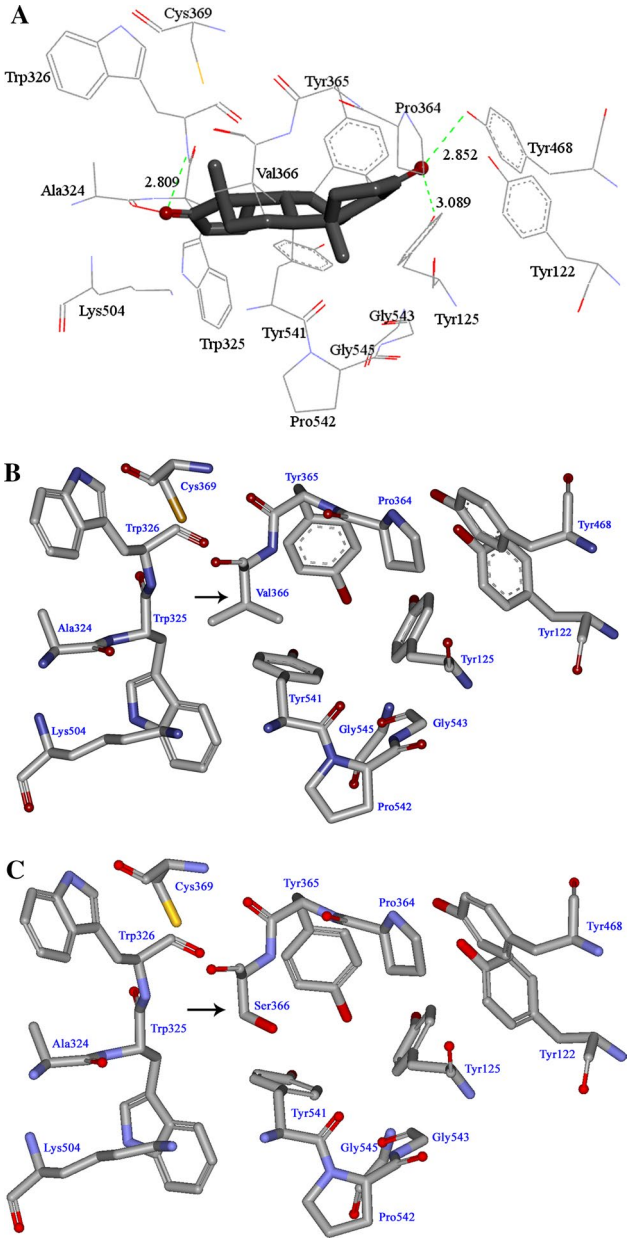

Fig. 7 Structure overview of $KSDD_I$ and $KSDD_{II}$. **a** The molecular docking of AD with the wide-type KSDD ($KSDD_I$). **b** Structure of substrate binding pocket in $KSDD_I$. **c** Structure of substrate binding pocket in $KSDD_{II}$

the AUTODOCK 4.2 program suite according to the previous study [31]. The docking input files were generated using the AutoDockTools program. A grid box size of 30 × 30 × 30 pointing in x, y and z directions was built. A grid spacing of 0.375 Å was used and fifty runs were generated for the best conformation. The O atoms in AD served as hydrogen bond acceptors forming three strong hydrogen bonding interactions with Tyr^{125}, Trp^{326} and Try^{468}. The distances of these hydrogen bonds were 3.089, 2.809 and 2.852 Å, respectively. Compared with the Val^{366} residue of

$KSDD_I$, the Ser^{366} residue of $KSDD_{II}$ has a hydroxyl group that could possibly interact with the active catalytic center by hydrogen bonding (Fig. 7c). Furthermore, due to steric hindrance, the two methyl groups of Val^{366} may interfere with the interaction of the substrate and the active center (Fig. 7b). In this way, the Val^{366} Ser mutation could possibly improve KSDD affinity toward AD and further enhance KSDD enzyme activity. Thus, the mutation of Val^{366} to Ser may directly affect the dehydrogenation activity of KSDD.

Purification of KSDD has been complicated by the presence of hydrophobic transmembrane domains which embed the enzyme in the membrane [8,15], and as a result progress in determining KSDD structure and its catalytic mechanism has been slow [29]. Oosterwijk et al. proposed a method for analyzing membrane protein structure and successfully revealed the crystal structure of Δ^4-(5α)-KSDD from *R. jostii* RHA1 [25]. Rohman et al. resolved the crystal structure of KSDD from *R. erythropolis* SQ1 and clarified its catalytic mechanism with the active site containing four key residues: Tyr^{119}, Tyr^{318}, Tyr^{487} and Gly^{491} [19]. Xie et al. revealed that Ser^{138} played an important role in maintaining the active center in the hydrophobic environment of KSDD [29]. Despite all these studies, the structure of KSDD from *M. neoaurum* remains unresolved. The analysis methods used for revealing the crystal structure of KSDD from *Rhodococcus* sp. could provide a feasible way for KSDD structural analysis in mycobacteria. In this study, the structural differences in KSDD caused by the mutation of Val^{366} to Ser^{366} resulted in obvious changes in the ADD/AD molar ratio between *M. neoaurum* ST-095 and *M. neoaurum* JC-12. This result suggested that, in addition to the identified active site residues, other amino acids such as Val^{366} are also important determinants of the $C_{1,2}$ dehydrogenation activity of the KSDD enzyme. This work provides a feasible way for analyzing the key amino acids of KSDD from *M. neoaurum* by site-directed mutagenesis. As the key residues of KSDD can greatly affect final ratios of products formed in industrial production strains [29], it is crucial to further identify the key residues to reveal the catalytic mechanism of the KSDD enzyme.

Conclusion

In this study, we clarified the different effects on ADD/AD molar ratio of strain *M. neoaurum* ST-095 and its mutant *M. neoaurum* JC-12 when used for phytosterol transformation. By PCR techniques and DNA sequence alignment, we found that the only difference between $KSDD_I$ and $KSDD_{II}$ was the change of Val^{366} to Ser^{366}. Enzyme assay of $KSDD_I$ and $KSDD_{II}$ showed that $KSDD_{II}$ activity was higher than $KSDD_I$, which indicated that the mutation could possibly enhance KSDD enzyme activity and improve the ADD/AD molar ratio. The analysis of the $KSDD_I$ and $KSDD_{II}$ functions in phytosterol bioconversion further verified that the differences in the ADD/AD molar ratio seen during phytosterol transformation by strains *M. neoaurum* ST-095 and *M. neoaurum* JC-12 were possibly due to the KSDD mutation. The KSDD structure analysis showed how the mutation in the amino acid sequence of KSDD might lead to KSDD structural modification and thereby result in the different KSDD enzyme activity, which in turn would alter the ADD/AD molar ratio.

Acknowledgments We sincerely appreciate Professor W. R. Jacobs, Jr. (Howard Hughes Medical Institute, USA) for providing plasmids pMV261 and pMV306, and Professor T. Parish (Department of Infectious & Tropical Diseases, United Kingdom) for providing plasmids of p2NIL and pGOAL19. This work was supported by the National Basic Research Program of China (973 Program) (2012CB725202), the High-Tech Research and Development Programs of China (2011AA02A211, SS2015AA021004), the National Natural Science Foundation of China (31570085), Jiangsu Province Science Fund for Distinguished Young Scholars (BK20150002), the Fundamental Research Funds for the Central Universities (JUSRP51306A), the 111 Project (111-2-06) and a Project Funded by the Priority Academic Program Development of Jiangsu Higher Education Institutions.

References

1. Anagnostopoulos C, Spizizen J (1961) Requirements for transformation in Bacillus subtilis. J Bacteriol 81:741
2. Bragin EY, Shtratnikova VY, Dovbnya D, Schelkunov M, Pekov YA, Malakho S, Egorova O, Ivashina T, Sokolov S, Ashapkin V (2013) Comparative analysis of genes encoding key steroid core oxidation enzymes in fast-growing Mycobacterium spp. strains. J Steroid Biochem Mol Biol 138:41–53
3. Choi K-P, Molnar I, Yamashita M, Murooka Y (1995) Purification and characterization of the 3-ketosteroid-Δ1-dehydrogenase of Arthrobacter simplex produced in Streptomyces lividans. J Biochem 117:1043–1049
4. Donova MV, Egorova OV (2012) Microbial steroid transformations: current state and prospects. Appl Microbiol Biotechnol 94:1423–1447. doi:10.1007/s00253-012-4078-0
5. Fernandes P, Cruz A, Angelova B, Pinheiro HM, Cabral JMS (2003) Microbial conversion of steroid compounds: recent developments. Enzyme Microb Technol 32:688–705. doi:10.1016/S0141-0229(03)00029-2
6. Fujii C, Morii S, Kadode M, Sawamoto S, Iwami M, Itagaki E (1999) Essential tyrosine residues in 3-Ketosteroid-Δ'-Dehydrogenase from Rhodococcus rhodochrous. J Biochem 126:662–667
7. Gordhan BG, Parish T (2001) Gene replacement using pretreated DNA. In: Parish T, Stoker NG (eds) *Mycobacterium tuberculosis* protocols, vol 54. Methods in Molecular Medicine. Humana Press Inc., New Jersey, pp 77–92. doi:10.1385/1-59259-147-7:077
8. Li Y, Lu F, Sun T, Du L (2007) Expression of ksdD gene encoding 3-ketosteroid-Δ^1-dehydrogenase from *Arthrobacter simplex* in *Bacillus subtilis*. Lett Appl Microbiol 44:563–568
9. Liu C, Zhang X, Z-m Rao, Shao M-l WuD, Z-h Xu, Li H (2015) Mutation breeding of high 4-androstene-3, 17-dione-producing Mycobacterium neoaurum ZADF-4 by atmospheric

and room temperature plasma treatment. J Zhejiang Univ Sci B 16:286–295
10. Long S, Zhang X, Rao Z, Chen K, Xu M, Yang T, Yang S (2016) Amino acid residues adjacent to the catalytic cavity of tetramer l-asparaginase II contribute significantly to its catalytic efficiency and thermostability. Enzyme Microb Technol 82:15–22. doi:10.1016/j.enzmictec.2015.08.009
11. Malaviya A, Gomes J (2008) Androstenedione production by biotransformation of phytosterols. Bioresour Technol 99:6725–6737. doi:10.1016/j.biortech.2008.01.039
12. Marsheck WJ, Kraychy S, Muir RD (1972) Microbial degradation of sterols. Appl Microbiol 23:72–77
13. Martin CK (1977) Microbial cleavage of sterol side chains. Adv Appl Microbiol 22:29–58
14. Matsushita H, Itagaki E (1992) Essential histidine residue in 3-ketosteroid-Δ1-dehydrogenase. J Biochem 111:594–599
15. Molnar I, Choi KP, Yamashita M, Murooka Y (1995) Molecular cloning, expression in Streptomyces livdans, and analysis of a gene cluster from Arthrobacter simplex encoding 3-ketosteroid-Δ1-dehydrogenase, 3-ketosteroid-Δ5-isomerase and a hypothetical regulatory protein. Mol Microbiol 15:895–905
16. Morii S, Fujii C, Miyoshi T, Iwami M, Itagaki E (1998) 3-Ketosteroid-Δ1-dehydrogenase of Rhodococcus rhodochrous: sequencing of the genomic DNA and hyperexpression, purification, and characterization of the recombinant enzyme. J Biochem 124:1026–1032
17. Murray HC, Peterson DH (1952) Oxygenation of steroids by Mucorales fungi. Google Patents
18. Plesiat P, Grandguillot M, Harayama S, Vragar S, Michel-Briand Y (1991) Cloning, sequencing, and expression of the Pseudomonas testosteroni gene encoding 3-oxosteroid delta 1-dehydrogenase. J Bacteriol 173:7219–7227
19. Rohman A, van Oosterwijk N, Thunnissen A-MW, Dijkstra BW (2013) Crystal structure and site-directed mutagenesis of 3-ketosteroid Δ1-dehydrogenase from Rhodococcus erythropolis SQ1 explain its catalytic mechanism. J Biol Chem 288:35559–35568
20. Shao M, Rao Z, Zhang X, Xu M, Yang T, Li H, Xu Z, Yang S (2015) Bioconversion of cholesterol to 4-cholesten-3-one by recombinant *Bacillus subtilis* expressing choM gene encoding cholesterol oxidase from *Mycobacterium neoaurum* JC-12. J Chem Technol Biotechnol 90:1811–1820. doi:10.1002/jctb.4491
21. Shao M, Zhang X, Rao Z, Xu M, Yang T, Li H, Xu Z (2015) Enhanced production of Androst-1, 4-Diene-3, 17-Dione by *Mycobacterium neoaurum* JC-12 using three-stage fermentation strategy. PLoS One 10:e0137658
22. Shao M, Zhang X, Rao Z, Xu M, Yang T, Li H, Xu Z, Yang S-T (2015) Efficient testosterone production by engineered Pichia pastoris co-expressing human 17β-hydroxysteroid dehydrogenase type 3 and Saccharomyces cerevisiae glucose 6-phosphate dehydrogenase with NADPH regeneration. Green Chem. doi:10.1039/C5GC02353J
23. Shen YB, Wang M, Li HN, Wang YB, Luo JM (2012) Influence of hydroxypropyl-β-cyclodextrin on phytosterol biotransformation by different strains of *Mycobacterium neoaurum*. J Ind Microbiol Biotechnol 39:1253–1259
24. Van der Geize R, Hessels G, Van Gerwen R, Vrijbloed J, Van der Meijden P, Dijkhuizen L (2000) Targeted disruption of the kstD gene encoding a 3-Ketosteroid Δ1-Dehydrogenase isoenzyme of rhodococcus erythropolis strain SQ1. Appl Environ Microbiol 66:2029–2036
25. van Oosterwijk N, Knol J, Dijkhuizen L, van der Geize R, Dijkstra BW (2012) Structure and catalytic mechanism of 3-ketosteroid-Δ4-(5α)-dehydrogenase from Rhodococcus jostii RHA1 genome. J Biol Chem 287:30975–30983
26. Wang Z, Zhao F, Chen D, Li D (2006) Biotransformation of phytosterol to produce androsta-diene-dione by resting cells of *Mycobacterium* in cloud point system. Process Biochem 41:557–561
27. Wang ZF, Huang YL, Rathman JF, Yang ST (2002) Lecithin-enhanced biotransformation of cholesterol to androsta-1, 4-diene-3, 17-dione and androsta-4-ene-3, 17-dione. J Chem Technol Biotechnol 77:1349–1357
28. Wei W, Wang FQ, Fan SY, Wei DZ (2010) Inactivation and augmentation of the primary 3-ketosteroid-Δ^1-dehydrogenase in *Mycobacterium neoaurum* NwIB-01: biotransformation of soybean phytosterols to 4-androstene-3,17-dione or 1,4-androstadiene-3,17-dione. Appl Environ Microbiol 76:4578–4582. doi:10.1128/aem.00448-10
29. Xie RL, Shen YB, Qin N, Wang YB, Su LQ, Wang M (2015) Genetic differences in ksdD influence on the ADD/AD ratio of *Mycobacterium neoaurum*. J Ind Microbiol Biotechnol:1–7
30. Xu XX, Jin FL, Yu XQ, Ji SX, Wang J, Cheng HX, Wang C, Zhang WQ (2007) Expression and purification of a recombinant antibacterial peptide, cecropin, from Escherichia coli. Protein Expr Purif 53:293–301
31. Xu Y-P, Qin J, Sun S-M, Liu T-T, Zhang X-L, Qian S-S, Zhu H-L (2014) Synthesis, crystal structures, molecular docking and urease inhibitory activity of nickel (II) complexes with 3-pyridinyl-4-amino-5-mercapto-1, 2, 4-triazole. Inorganica Chim Acta 423:469–476
32. Yao K, Xu L-Q, Wang F-Q, Wei D-Z (2014) Characterization and engineering of 3-ketosteroid-△1-dehydrogenase and 3-ketosteroid-9α-hydroxylase in Mycobacterium neoaurum ATCC 25795 to produce 9α-hydroxy-4-androstene-3,17-dione through the catabolism of sterols. Metab Eng 24:181–191. doi:10.1016/j.ymben.2014.05.005
33. Zhang WQ, Shao ML, Rao ZM, Xu MJ, Zhang X, Yang TW, Li H, Xu ZH (2013) Bioconversion of 4-androstene-3,17-dione to androst-1,4-diene-3,17-dione by recombinant *Bacillus subtilis* expressing ksdd gene encoding 3-ketosteroid-Δ^1-dehydrogenase from *Mycobacterium neoaurum* JC-12. J Steroid Biochem Mol Biol 135:36–42. doi:10.1016/j.jsbmb.2012.12.016
34. Zhong C, Rao Z, Xia H, Xu Z, Fang H, Zhuge J (2009) Mutation breeding of *Mycobacterium* sp. for transformation of phytosterol into androst-1,4-diene-3,17-dione. Chem Bioeng 7:43–46 **(in Chinese)**